AN ANISOTROPIC NONLOCAL CONVECTION THEORY

L. DENG,[1] D. R. XIONG,[2] AND K. L. CHAN[3]

ABSTRACT

We present in this paper an anisotropic nonlocal theory of stellar convection. Following the idea of Rotta, we propose that the correlation of turbulent pressure and velocity gradient tends to make the turbulent velocity isotropic, and we further introduce a convection parameter c_3 to measure the strength of such isotropization. By using such a theory, the structure of the solar convection zone is calculated. Our calculation shows that the radial component dominates in the convectively unstable zone, in which the ratio between the radial component and the horizontal component is $w_r^2/w_h^2 = (3 + c_3)/2c_3$. In the upper overshooting zone, turbulent velocity is almost isotropic ($w_r^2/w_h^2 \sim 0.5$) and is independent of c_3, while in the lower overshooting zone, $w_r^2/w_h^2 \leq 0.5$, and it tends to decrease as c_3 decreases. We also studied the effects of anisotropic convection on the structure and evolution of stars. It is shown that the anisotropy hardly affects the temperature and pressure structure of stars. However, the anisotropy increases with the decrease of c_3; therefore, the effect of overshooting decreases. Thus, the effects of anisotropy of turbulent convection on stellar evolution cannot be neglected.

Subject headings: convection — stars: evolution

1. INTRODUCTION

Convection is an internal instability of gravitationally stratified matter. When the local temperature gradient exceeds the adiabatic value, a perturbed fluid element will be accelerated by buoyant force along the direction of gravity, and convection sets in at such a condition. The original direction of convective motion is aligned with gravity, i.e., the radial direction in the stellar internal convective zone. Due to the continuity and nonlinearity of fluid kinetics, a part of the kinetic energy of a convective element originated from buoyant force will be converted into that of horizontal motion. In the local mixing-length theory of convection (Böhm-Vitense 1958), the kinetic energy in the horizontal motion of an element is supposed to be the same as that in the radial direction. Similar assumptions have been adopted in all other theories of stellar convection. A direct hydrodynamical simulation should be able to provide a more reliable diagnosis for such a problem. However, a three-dimensional hydrodynamical simulation will not be ready for the calculation of stellar evolution models in the foreseeable future due to the enormous demand of computational power. We believe that a simple anisotropic nonlocal theory of convection will be more feasible and realistic to deal with stellar evolutionary modeling, while hydrodynamical simulations can be used to constrain the parameters adopted by the theory and the results coming out of such models.

Following such a consideration, we have presented a method dealing with the anisotropy of stellar turbulent convection (Xiong et al. 1997), which is applied here to model the structure of the solar convective zone. In order to find out how such a simple treatment behaves in describing the general properties of the anisotropy of the turbulent convection, we have compared our results with the observations of the velocity field of solar granules and the results of dynamical simulations. In § 2 the treatment of anisotropy of turbulent convection is presented together with the working

equations of our numerical calculations. The results on the structure of the solar convection zone are given in § 3, with which the effects of anisotropy on the structure of the solar (stellar) convection zone and lithium depletion are studied. The comparisons between our model and the observed velocity field of solar granule and hydrodynamical simulations are presented in §§ 3.4 and 3.5. Conclusions of the present work and discussions are given in § 4.

2. A TREATMENT OF THE ANISOTROPY OF TURBULENCE AND THE WORKING EQUATIONS OF STELLAR STRUCTURE

The stellar convection theory we presented so far (Xiong 1977, 1978, 1979, 1980, 1989a) is a dynamic theory of auto- and cross-correlation functions of turbulent velocity and temperature fluctuations; the most complicated part is the pressure fluctuations. In the papers mentioned above, it is assumed that the only function of pressure fluctuations p' is to impel the turbulence toward isotropic; all of their other effects can be neglected. We are going to concentrate on the treatment of pressure fluctuations and the anisotropy of turbulent convection in this paper; a full scope of our convection theory can be found in Xiong et al. (1997). Starting from the hydrodynamic equations of fluid and by some elaborating manipulations, the dynamic equations of the second-order correlation of turbulent velocity can be given as follows:

$$
\begin{aligned}
&\frac{D}{Dt}\overline{w'^i w'^j} + \overline{w'^i w'^k}\nabla_k \bar{u}^j + \overline{w'^j w'^k}\nabla_k \bar{u}^i \\
&+ \frac{1}{\bar{\rho}}\nabla_k\left(\bar{\rho}\overline{u'^k w'^i w'^j}\right) - \bar{B}\overline{w'^i}\frac{T}{\bar{T}}\left(\frac{D\bar{u}^j}{Dt} + g^{jk}\nabla_k\bar{\phi}\right) \\
&- \bar{B}\overline{w'^j\frac{T'}{\bar{T}}}\left(\frac{D\bar{u}^i}{Dt} + g^{ik}\nabla_k\bar{\phi}\right) \\
&+ \frac{1}{\bar{\rho}}\nabla\left[g^{ik}\overline{w'^j p'} + g^{jk}\overline{w'^i p'} - \overline{w'^i \sigma^{jk}(u')} - \overline{w'^j \sigma^{ik}(u')}\right] \\
&- \frac{1}{\bar{\rho}}\left(g^{ik}\overline{p'\nabla_k w'^j} + g^{jk}\overline{p'\nabla_k w'^i}\right) \\
&= -\frac{1}{\bar{\rho}}\left[\overline{\sigma^{jk}(u')\nabla_k w'^i} + \overline{\sigma^{ik}(u')\nabla_k w'^j}\right],
\end{aligned}
\tag{1}
$$

[1] National Astronomical Observatories, Chinese Academy of Sciences, A20 Datun Road, Chaoyang Beijing 100012, China; licai@bao.ac.cn.
[2] Purple Mountain Observatory, Chinese Academy of Sciences, 2 Beijing Xi Lu, Nanjing, Jiangsu 210008, China; xiongdr@pmo.ac.cn.
[3] Department of Mathematics, Hong Kong University of Science and Technology, Clear Water Bay, Kowloon, Hong Kong, China; maklchan@ust.hk.

where $D/Dt = \partial/\partial t + \bar{u}^k \nabla_k$ is the comoving differential operator, P is the pressure, T is the temperature, ρ is the density, u^i is the i component of velocity, ϕ is the gravitational potential, $\sigma^{ik}(u)$ is the viscosity tensor, and $B = (\partial \ln \rho/\partial \ln T)_P$ is the expansion coefficient. The physical quantities with an overhead bar are the average values of the corresponding ones, while the ones with a prime are their fluctuations, for instance,

$$P = \bar{P} + p', \quad \rho = \bar{\rho} + \rho', \quad T = \bar{T} + T', \quad u^i = \bar{u}^i + u'^i.$$

As for the definition of average value, for normal physical quantities such as pressure and density, the average values of their turbulent fluctuations vanish,

$$\bar{p}' = \bar{\rho}' = 0,$$

but for temperature T and velocity u^i, the averages are weighted by density, so that

$$\overline{\rho T} = \bar{\rho}\bar{T}, \quad \overline{\rho u^i} = \bar{\rho}\bar{u}^i, \quad w'^i = \overline{\rho u'^i}/\bar{\rho};$$

however,

$$\overline{\rho T'} = 0, \quad T' = -\frac{1}{\bar{\rho}}\overline{\rho' T'} \neq 0,$$

$$\overline{\rho u'^i} = \bar{\rho}\bar{w}'^i = 0, \quad \bar{u}'^i = \frac{1}{\bar{\rho}}\overline{\rho' u'^i} \neq 0.$$

Such a method of density-weighted averaging is physically sound: $\overline{\rho u'^i} = 0$, for instance, means that there is no bulk motion of matter in convection. Besides, it brings about great convenience in the whole treatment; the continuity equation of fluid keeps its regular form in this case. Otherwise, very bothersome terms such as $\overline{\rho' u'^i}$ would show up. Similarly for the mean energy equation, the original form is retained except for the convective energy transport term. In the convection theory of Canuto (1993), the so-called non-Boussinesq terms were used. When using the density-weighted mean of velocity defined above, many non-Boussinesq terms of Canuto (1993) disappear automatically. This issue has been carefully addressed by several previous studies (Xiong 1978, 1989a; Xiong & Deng 1997; Canuto 1997). In this work, instead of applying the so-called Boussinesq approximation normally used in convection theories, we would like to use a softer anelastic approximation, i.e.,

$$\frac{D}{Dt}\left(\frac{\rho'}{\bar{\rho}}\right) - \frac{1}{\bar{\rho}}\nabla_k\left(\overline{\rho u'^k}\right) = 0.$$

As shown in an early study by Gough (1969) and Latour et al. (1976), the physics underlying the anelastic approximation is to filter out the high-frequency acoustic waves in convective motions. Assuming that the relative fluctuations in density and temperature are small, acoustic waves become negligible and therefore can be excluded. It should made clear that our treatment is strictly limited to the case of the subsonic regime of convection.

In order to solve the problem in spherical coordinates, equation (1) has been written using tensors, where g^{ik} is the metric tensor, and the implicit notation of summation is adopted, i.e., a pair of subscripts and superscripts means summation with respect to that script from 1 to 3. In the derivation of equation (1), we have used the subsonic hypothesis, i.e., $|\rho'/\bar{\rho}| \ll 1$. Truncated at the first order of $|\rho'/\bar{\rho}|$, equation (1) is accurate, and no other simplification or assumptions have been applied. Here

$\bar{\rho}\overline{w'^i w'^j}$ is the Reynolds stress of turbulence, which can be decomposed into an isotropic component (turbulent press) $\bar{\rho}x^2$ and an anisotropic one $\rho\mathcal{A}^{ij}$; therefore,

$$\overline{w'^i w'^j} = g^{ij}x^2 + \mathcal{A}^{ij}, \tag{2}$$

where

$$x^2 = g_{\alpha\beta}\overline{w'^\alpha w'^\beta}/3, \tag{3}$$

$$g_{\alpha\beta}\mathcal{A}^{\alpha\beta} = 0. \tag{4}$$

Inserting equation (2) into equation (1) and contracting with respect to indices i and j, the dynamic equation for the isotropic component of Reynolds stress can be derived as

$$\begin{aligned}
&\frac{Dx^2}{Dt} + \frac{2}{3}\left(x^2\nabla_k u^k + \mathcal{A}^{ik}\nabla_k\bar{u}_i\right) \\
&+ \frac{1}{3\bar{\rho}}\nabla_k\left[\overline{\bar{\rho}u'^k w_i w'^i} + 2\overline{p'w'^k} - 2\overline{w_i \sigma^{ik}(u')}\right] \\
&- \frac{2}{3}\bar{B}\overline{w'^k \frac{T'}{\bar{T}}}\left(\frac{D\bar{u}_k}{Dt} + \nabla_k\bar{\phi}\right) - \frac{2}{3\bar{\rho}}\overline{p'\nabla_k w'^k} \\
&= -\frac{2}{3\bar{\rho}}\overline{\sigma^{ik}(u')\nabla_k w_i}. \tag{5}
\end{aligned}$$

Subtracting the production of g^{ij} and equation (5) from equation (1), one has the dynamic equation of the anisotropic component of Reynolds stress $\mathcal{A}^{ij}$,

$$\begin{aligned}
&\frac{D\mathcal{A}^{ij}}{Dt} + x^2\left(g^{ik}\nabla_k\bar{u}^j + g^{jk}\nabla_k\bar{u}^i - \frac{2}{3}g^{ij}\nabla_k\bar{u}^k\right) \\
&+ \left(\mathcal{A}^{ik}\nabla_k\bar{u}^j + \mathcal{A}^{jk}\nabla_k\bar{u}^i - \frac{2}{3}g^{ij}\mathcal{A}^{kl}\nabla_k\bar{u}_l\right) \\
&+ \frac{1}{\bar{\rho}}\nabla_k\left[\overline{\bar{\rho}u'^k \mathcal{A}^{ij}} + \overline{(g^{ik}w'^j + g^{jk}w'^i)p'}\right. \\
&\left. - \frac{2}{3}g^{ij}\overline{p'w'^k} - \overline{w'^i\sigma^{jk}(u')} - \overline{w'^j\sigma^{ik}(u')} + \frac{2}{3}g^{ij}\overline{w_l\sigma^{kl}(u')}\right] \\
&- \bar{B}\left(g^{ik}\overline{w'^j\frac{T'}{\bar{T}}} + g^{jk}\overline{w'^i\frac{T'}{\bar{T}}} - \frac{2}{3}g^{ij}\overline{w'^k\frac{T'}{\bar{T}}}\right)\left(\frac{D\bar{u}_k}{Dt} + \nabla_k\bar{\phi}\right) \\
&- \frac{1}{\bar{\rho}}\overline{p'\left(g^{ik}\nabla_k w'^j + g^{jk}\nabla_k w'^i - \frac{2}{3}g^{ij}\nabla_k w'^k\right)} \\
&= -\frac{1}{\bar{\rho}}\left[\overline{\sigma^{ik}(u')\nabla_k w'^j} + \overline{\sigma^{jk}(u')\nabla_k w'^i} - \frac{2}{3}g^{ij}\overline{\sigma^{lk}(u')\nabla_k w_l}\right]. \tag{6}
\end{aligned}$$

Multiplying equation (5) with $3\bar{\rho}/2$, we have

$$\begin{aligned}
\frac{3}{3}\bar{\rho}\frac{Dx^2}{Dt} = &-\bar{\rho}\left(x^2\nabla_k\bar{u}^k + \mathcal{A}^{ik}\nabla_k\bar{u}_i\right) \\
&- \nabla_k\left[\overline{\bar{\rho}u'^k w_i w'^i}/2 + \overline{p'w'^k} - \overline{w'^i\sigma^{ik}(u')}\right] \\
&+ B\bar{\rho}\overline{w'^k\frac{T'}{\bar{T}}}\left(\frac{D\bar{u}_k}{Dt} + \nabla_k\bar{\phi}\right) + \overline{p'w'^k} - \overline{\sigma^{ik}(u')\nabla_k w'^i}. \tag{7}
\end{aligned}$$

Equations (5) and (7) are in fact the conservation equations of turbulent kinetic energy. The left-hand side of equation (7) is the rate of variation in time of turbulent kinetic energy per unit volume, which is the sum of all of the right-hand side terms: the first term on the right-hand side is the energy transformation rate from the ordered mean motion into that of turbulence through the deformation of fluid (or otherwise named turbulent viscosity); the second term (the divergence term) is the total gaining rate of turbulent kinetic energy from the turbulent kinetic energy flux ($\bar{\rho}u'^k w_i w'^i/2$), the turbulent stress flux ($p'w'^k$), and viscous stress flux [$\overline{w_i \sigma^{ik}(u')}$] crossing the boundary of the fluid element; the third term is the gaining rate of turbulent kinetic energy through the work done by buoyant force; while the fourth term is the rate of transformation from acoustic wave energy into turbulent kinetic energy through the work done by pressure fluctuations. The main contributions to all of these terms are from low wavenumbers (or large turbulent eddies). The last term on the right-hand side of equation (7) is the transformation rate from kinetic energy into thermal energy due to molecular viscosity, which takes place in high wavenumbers (small turbulent eddies). As such, what equations (5) and (7) describe is a picture of energy balance of turbulent convection: large-scale eddies extract energy from the mean fluid field through buoyant force and the deformation and sharing of fluid. Due to the nonlinear nature of fluid motion, turbulent kinetic energy is cascaded gradually from low to high wavenumbers and is eventually transformed by molecular viscosity into thermal energy of media at the high-wavenumber end. Following the theory of isotropic turbulence, the viscous dissipation term could be expressed as (Hinze 1975; Xiong 1978)

$$\frac{1}{\bar{\rho}} \overline{\sigma^{ik}(u')\nabla_k w_i} = 2\eta_e k_e x^3 = 2\sqrt{3}\eta_e k_{e1} x^3 = \frac{1.56}{l_{e1} x^3}, \quad (8)$$

where η_e is the Heisenberg eddy coupling constant, adopted as $\eta_e = 0.45$ in this work, and k_e is the wavenumber of energy-containing eddies whose radial linear dimension is $l_{e1} = 1/k_{e1}$. Normally such linear dimension is assumed to be proportional to pressure (or density) scale height,

$$l_{e1} = c_1 H_P = c_1 \frac{r^2 p}{GM_r \rho}. \quad (9)$$

Equation (9) is of course a working assumption. In our statistical theory of turbulent convection, the convection parameter c_1 corresponds to the mixing-length parameter $\alpha = l/H_P$ in the mixing-length theory of convection, which determines the efficiency of convective energy transport. The calibration of c_1 is normally done through a comparison of modeling and observations of the internal structure of the Sun and evolution of stars. However, the parameter c_1 is very unlikely to be a universal constant. It depends on the mass, luminosity, and effective temperature of stars under consideration. Indeed, this is still a very important source of uncertainty in the current theory of stellar convection. Apart from the usual constraints such as the standard solar model calibration and lithium abundance constraint, a three-dimensional hydrodynamic simulation should provide a supplementary reference to the use of such an adjustable parameter c_1 (Ludwig et al. 1999). Furthermore, the parameter c_1, instead of being a constant for a given star, should be very likely a function of stellar radius. Fortunately, convection is extremely efficient in energy transport at the deep interior of stars, where the temperature gradient is almost adiabatic regardless of the

choice of the parameter c_1. The depth of the surface convection region, however, depends primarily on the structure of the superadiabatic zone at the top of the region. Therefore, the structure of the surface convective region is mainly fixed by the choice of c_1 in the top superadiabatic zone, which has nothing to do with the c_1 adopted for the deep interior. For the internal thermal structure of stars, c_1 and its variation in the deep interior are not important.

The term $\overline{\bar{\rho}u'^k w_i w'^i}/2$ in equation (7) is turbulent kinetic energy flux, whose ratio with respect to convective thermal (enthalpy) flux is about the same order of magnitude as M^2, where $M = x/C_s$ is the Mach number of turbulent convective motion. In the deep interior of stars, $M \ll 1$. Hence, compared with convective thermal flux, turbulent kinetic energy flux can hardly affect the structure of stars in terms of energy transport and is therefore negligible (Xiong 1986). Although being very small, one cannot generally ignore turbulent kinetic energy flux because it represents the nonlocal effect of convection. Once it is ignored, the statistical theory of turbulent convection goes back to the local expression (Xiong 1980, 1989a). In our theory, a gradient type of diffusion approximation is adopted, in which the third-order correlations are expressed in terms of the second-order ones,

$$\overline{u'^k w_i w'^i} = -g^{k\alpha} x \Lambda \nabla_\alpha \overline{w_i w'^i}$$
$$= -3g^{k\alpha} x \Lambda \nabla_\alpha x^2, \quad (10)$$

where Λ is the diffusion length of turbulence, and following the theory of turbulence (Hinze 1975), it is

$$\Lambda = 3/4k_e = \sqrt{3}/4k_{e1} = \sqrt{3}\Lambda_1/4.$$

In a similar way as to express turbulent dissipation, we assume that Λ_1 is proportional to the local pressure scale height H_P, so that

$$\Lambda = \frac{\sqrt{3}\Lambda_1}{4} = \frac{\sqrt{3}}{4} c_2 H_P = \frac{\sqrt{3}c_2 r^2 P}{4GM_r \rho}.$$

Parameter c_2 introduced here is a convection parameter linked with the nonlocal turbulent diffusion in our statistical theory of convection, where the distance of convective overshooting is in general proportional to $(c_1 c_2)^{1/2}$ but can be different for different physical quantities by a factor of order unity (Xiong 1986; Xiong & Deng 2002).

Equation (10) represents isotropic turbulent diffusion. For anisotropic turbulence, the coefficient of turbulent diffusion changes with the direction. Our approach in this case is the following:

$$\overline{u'^k w_i w'^i} = -3\left(g^{k\alpha} x^2 + \mathcal{A}^{k\alpha}\right)^{1/2} \Lambda \nabla_\alpha x^2. \quad (11)$$

Based on order-of-magnitude analysis, we have $\nabla_k \overline{[w_i \sigma^{ik}(u')]}/\overline{\sigma^{ik}\nabla_k w_i} \sim l_d/l \ll 1$ and $\nabla_k(\overline{p'w'^k})/\overline{p'\nabla_k w'^k} \sim l_e/l \leq 1$, where l is the characteristic length of the mean field of fluid and l_d is that of turbulent dissipation eddies. The term $-\overline{p'\nabla_k w'^k} \sim p'(d/dr)(\rho'/\bar{\rho})$ represents the transformation rate from turbulent kinetic energy into that of sound waves at high frequencies. For subsonic convective flow, this term can be neglected, and this is actually what the inelastic approximation is all about. Based on the order-of-magnitude analysis of the terms in equation (7) and

using equations (8)–(11), we can give the conservation equation for turbulent kinetic energy in the case of quasi-static convection ($\bar{u}^i = 0$),

$$\frac{\partial x^2}{\partial t} - \frac{\partial}{\partial M_r}\left(Q\frac{\partial x^2}{\partial M_r}\right) + \frac{2}{3}\frac{GM_r}{r^2}\left(1.56\frac{\rho x^3}{c_1 P} - BV\right) = 0,$$
(12)

where

$$Q = \frac{4\sqrt{3}\pi^2 c_2 r^6 \rho P\left(x^2 + \mathcal{A}^{11}\right)^{1/2}}{GM_r},$$
$$V = \overline{w'^1 T'}/\bar{T}.$$
(13)

For quasi-static convection, the first term on the left-hand side of equation (12) should not show up according to the above discussion; the only argument to keep it is for the stability of numerical calculations. After a large enough number of time steps, the structure of the convective zone approaches its static state, and that term vanishes naturally at this condition.

Parameter $\mathcal{A}^{ij}$ is the anisotropic component of turbulent Reynolds stress; therefore, equation (6) can also be regarded as the energy conservation equation for the anisotropic component of turbulence. Following the original definitions (eqs. [2]–[4]), the sum of all anisotropic components vanishes. As such, equation (6) in fact describes the transformation among the anisotropic components. In the case of quasi-static convection, the only drive is buoyant force from which a turbulent eddy gains its radial kinetic energy. Due to continuation of fluid and the nonlinear interactions among turbulent eddies, a part of radial turbulent kinetic energy is converted into that of horizontal motion. As pointed out by Rotta (1951), the correlation of pressure and velocity gradient tends to make turbulence isotropic, so that we assume

$$\frac{1}{\rho}\overline{p'\left(g^{ik}\nabla_k w'^j + g^{jk}\nabla_k w'^i - \frac{2}{3}g^{ij}\nabla_k w'^k\right)}$$
$$= -c_3 \frac{4\sqrt{3}\eta_e GM_r \rho x}{3c_1 r^2 P}\mathcal{A}^{ij}.$$
(14)

Parameter c_3 introduced here is a convection parameter used to describe the anisotropy of turbulence. A more complex approximation incorporating the Rotta terms was also used in Canuto (1993). For increasing c_3, the correlation term of the pressure and velocity gradient is more and more capable of making turbulence isotropic, and the turbulence becomes more and more isotropic in this case (we further discuss this point below).

The right-hand side of equation (6) is the viscous dissipation term, which can be expressed as, in a similar way as for equation (8),

$$\frac{1}{\rho}\left[\overline{\sigma^{ik}(u')\nabla_k w'^j} + \overline{\sigma^{jk}(u')\nabla_k w'^i} - \frac{2}{3}g^{ij}\overline{\sigma^{\alpha\beta}(u')\nabla_\alpha w'^\beta}\right]$$
$$= \frac{4\sqrt{3}\eta_e GM_r \rho x}{3c_1 r^2 P}\mathcal{A}^{ij},$$
(15)

where $\overline{u'^k \mathcal{A}^{ij}}$ is the nonlocal convective flux of the anisotropic component of Reynolds stress, which can be expressed, in a

similar way as for equation (11) under the condition of anisotropic diffusion approximation, as follows:

$$\overline{u'^k \mathcal{A}^{ij}} = -\left(g^{k\alpha}x^2 + \mathcal{A}^{k\alpha}\right)^{1/2}\Lambda\nabla_\alpha \mathcal{A}^{ij}.$$
(16)

In a quasi-static situation, $\mathcal{A}^{ij}$ possesses only three (diagonal) components different from zero; all other elements will vanish. In a spherical coordinate frame, $(x_1, x_2, x_3) = (r, \theta, \phi)$; then it follows from equation (4) that

$$r^2\mathcal{A}^{22} = r^2\sin^2\theta\mathcal{A}^{33} = -\mathcal{A}^{11}/2.$$

In fact, $\mathcal{A}^{ij}$ has only one ($\mathcal{A}^{11}$) independent component different from zero. Following the same argument of order-of-magnitude analysis, it can also be proved that the pressure stress flux and viscous stress flux terms in equation (6) are small in comparison with other terms and therefore can be neglected. Inserting equations (14), (15), and (16) into equation (6), we can derive the conservation equation for the component $\mathcal{A}^{11}$ with some simple manipulations,

$$\frac{\partial \mathcal{A}^{11}}{\partial t} - \frac{\partial}{\partial M_r}\left(Q\frac{\partial \mathcal{A}^{11}}{\partial M_r}\right) + \left[\frac{2}{3}\frac{1.56(1+c_3)GM_r \rho x}{c_1 Pr^2} + S\right]\mathcal{A}^{11}$$
$$- \frac{4}{3}\frac{GM_r}{r^2}BV = 0,$$
(17)

where

$$S = \frac{3\sqrt{3}c_2 P\left(x^2 - \mathcal{A}^{11}/2\right)^{1/2}}{2GM_r \rho},$$
(18)

which turns up because of the term $\nabla_k(\overline{\rho u'^k \mathcal{A}^{11}})$ in equation (6) when considering the spherical coordinate.

Equations (12) and (17) are, respectively, the nonlocal convection equations for the isotropic component x^2 and the independent anisotropic component $\mathcal{A}^{11}$ of the autocorrelations of turbulent velocity, under quasi-static condition. In a similar way, the nonlocal convection equations for the autocorrelation of turbulent temperature $Z = \left(\overline{T'/\bar{T}}\right)$ and the cross-correlation of the radial component of turbulent velocity and temperature fluctuation $V = \overline{w'^1 T'}/\bar{T} = \overline{w'_r T'}/\bar{T}$ can be derived, which are the following:

$$\frac{\partial Z}{\partial t} - \frac{1}{\rho C_p^2}\frac{\partial}{\partial M_r}\left(\rho C_p^2 Q\frac{\partial Z}{\partial M_r}\right)8\pi r^2 \rho V\left(\frac{\partial \ln T}{\partial M_r} - \nabla_{ad}\frac{\partial \ln P}{\partial M_r}\right)$$
$$+ 1.56\frac{GM_r \rho}{c_1 r^2 P}(x + x_c)Z = 0,$$
(19)

$$\frac{\partial V}{\partial t} - \frac{1}{C_p}\frac{\partial}{\partial M_r}\left(C_p Q\frac{\partial V}{\partial M_r}\right)$$
$$+ 8\pi r^2 \rho\left(x^2 + \mathcal{A}^{11}\right)\left(\frac{\partial \ln T}{\partial M_r} - \nabla_{ad}\frac{\partial \ln P}{\partial M_r}\right) + \frac{S}{3}V$$
$$+ \frac{GM_r}{r^2}\left[0.78(3x + x_c)\left(1 + \frac{\Pi^{11}}{x^2}\right)^{-1/2}\frac{\rho V}{c_1 P} - BZ\right] = 0,$$
(20)

where $x_c = 3acGM_r T^3/c_1\rho C_P \kappa r^2 P$ and $x/x_c = P_e$ is the effective Peclet number of turbulent convection. The conservation

equations of mass, energy, and momentum (hydrostatic equilibrium) and the equation of radiative energy transfer for stellar structure can be written as

$$\frac{\partial r^3}{\partial M_r} = \frac{3}{4\pi\rho}, \tag{21}$$

$$\frac{\partial}{\partial M_r}\left(P + \rho x^2\right) + \frac{1}{r}\frac{\partial}{\partial M_r}\left(r^3\rho\mathcal{A}^{11}\right) = -\frac{GM_r}{4\pi r^4}, \tag{22}$$

$$\frac{\partial}{\partial M_r}(L_r + L_c + L_t) = \varepsilon_N, \tag{23}$$

$$\frac{\partial T^4}{\partial M_r} = -\frac{3\kappa L_r}{16\pi^2 acr^4}, \tag{24}$$

where ε_N is the nuclear energy generation rate (energy carried by neutrino is subtracted), κ is the opacity, c is the speed of light, and a is the radiation constant. L_r, L_c, and L_t are, respectively, the luminosities corresponding to radiative flux, convective thermal (enthalpy) flux, and turbulent kinetic energy flux,

$$L_r = 4\pi r^2 F_r = -\frac{16\pi^2 acr^4}{3\kappa}\frac{\partial T^4}{\partial M_r}, \tag{25}$$

$$L_c = 4\pi r^2 \rho C_P T V, \tag{26}$$

$$L_t = -\frac{3}{2}Q\frac{\partial x^2}{\partial M_r}. \tag{27}$$

When modeling the envelope structure of stars, $\varepsilon_N = 0$, equation (23) may be simplified as

$$L_r + L_c + L_t = L_0, \tag{28}$$

where L_0 is the total stellar luminosity. Equations (12), (17), (19), (20), (21), (22), (24), and (28) form a closed system of equations of envelope structure of stars in the framework of anisotropic nonlocal convection. Setting both upper and lower boundaries in the corresponding overshooting zones, the boundary conditions are

$$r = R_0, \tag{29}$$

$$P = P_0, \tag{30}$$

$$T = T_0, \tag{31}$$

$$\frac{\partial x}{\partial M_r} = -\beta_+ \frac{GM_0 x}{4\pi R_0^4 P}, \tag{32}$$

$$\frac{\partial Z}{\partial M_r} = -(2\beta_+ - \nabla)\frac{GM_0 Z}{4\pi R_0^4 P}, \tag{33}$$

$$\frac{\partial V}{\partial M_r} = -(3\beta_+ - \nabla)\frac{GM_0 V}{4\pi R_0^4 P}, \tag{34}$$

and

$$\frac{\partial \mathcal{A}^{11}}{\partial M_r} = -\beta_+ \frac{GM_0 \mathcal{A}^{11}}{4\pi R_0^4 P} \tag{35}$$

at the surface ($M_r = M_0$) and

$$\frac{\partial x}{\partial M_r} = -\beta_- \frac{GM_b x}{4\pi r^4 P}, \tag{36}$$

$$\frac{\partial Z}{\partial M_r} = -(2\beta_- - \nabla)\frac{GM_b Z}{4\pi r^4 P}, \tag{37}$$

$$\frac{\partial V}{\partial M_r} = -(3\beta_- - \nabla)\frac{GM_b V}{4\pi r^4 P}, \tag{38}$$

and

$$\frac{\partial \mathcal{A}^{11}}{\partial M_r} = -\beta_- \frac{GM_b \mathcal{A}^{11}}{4\pi r^4 P} \tag{39}$$

at the bottom ($M_r = M_b$), where

$$\beta_{\pm} = -\frac{\nabla - 0.3}{2.4} \pm \sqrt{\left(\frac{\nabla - 0.3}{2.4}\right)^2 + \frac{0.5 - \nabla}{6} + \frac{2\sqrt{3}\eta_e + 1}{3\sqrt{3}c_1 c_2}}. \tag{40}$$

At the surface boundary, the convective variables decrease toward the surface, and the positive solution β_+ is adopted. While at the bottom boundary of the convective zone, those variables decrease toward the center too, and the negative solution β_- is used. The boundary conditions given by equations (32)–(39) are derived by the asymptotic analytic solutions of the power-law decreasing convective variables x, Z, V, and $\mathcal{A}^{11}$ with respect to pressure P in the overshooting zone (Xiong 1989b).

Inside the convective zone (far away from the boundary of the zone), the terms including the third-order correlation representing the effect of nonlocal convection (i.e., terms containing Q and S) in equations (12) and (17) are negligible compared with the second-order terms. For static convection, we have

$$\mathcal{A}^{11} \approx \frac{c_1 PV}{0.78(1 + c_3)\rho x} \approx \frac{2x^2}{1 + c_3}. \tag{41}$$

Therefore, it follows for the interior of the convective zone that the ratio between the mean squared radial component turbulent velocity (w_r^2) and that of the horizontal one (w_h^2) is approximately

$$\frac{w_r^2}{w_h^2} = \frac{x^2 + \mathcal{A}_1^1}{2x^2 + \mathcal{A}_2^2 + \mathcal{A}_3^3}$$

$$\approx \frac{1 + [2/(1 + c_3)]}{2 - [2/(1 + c_3)]} = \frac{3 + c_3}{2c_3}. \tag{42}$$

The radial and horizontal components of turbulent velocities are defined as the square roots of the corresponding quantities [$w_r = (w_r^2)^{1/2}$, $w_h = (w_h^2)^{1/2}$], whose ratio as a function of the convective parameter c_3 is given in Table 1. The first column gives the value of c_3, the second column presents a ratio predicted by the analytic formula given by equation (42), while the third column presents the numerical results calculated for the solar convective zone; the two sets of values are very close. This verifies again that inside the convective zone far away from the boundary, the third-order correlations are truly negligible compared with the second-order ones, in that their nonlocal convection is close to the local one. It is worth being pointed out again that, generally speaking, local convection and nonlocal convection are different, and this

TABLE 1
The Ratio of the Radial Component of Turbulent Velocity to the Horizontal One versus the Convective Parameter c_3

c_3	w_r^2/w_h^2 Equation (42)	w_r^2/w_h^2 Numerical
1	2.00	2.00
2	1.25	1.25
3	1.00	1.00
7	0.714	0.715
15	0.600	0.600
31	0.548	0.549
63	0.523	0.524
127	0.509	0.512
255	0.502	0.506

is especially the case near the boundary of the convective zone and within the overshooting regions, where overshooting effects dominate.

3. THE RESULTS OF NUMERICAL CALCULATIONS

The goal of this work is to study the effects of the anisotropy of turbulent convection on the structure and evolution of stars. Being the nearest star, the Sun is an ideal target of our purpose. As demonstrated in the previous section, there are three convective parameters in our theory, c_1, c_2, and c_3, explicitly described as follows:

1. Parameter c_1 is the one that is linked with the turbulent dissipation process, whose primary function is to determine the efficiency of convective energy transport. For growing c_1, turbulent dissipation decreases. With given c_2 and c_3, the surface convective zone gets deeper for larger c_1. Under a local convection approximation, our theory gives about the same efficiency of energy transport as the original Vitense theory when $c_1 = 2.9\alpha$, where α is the normal mixing-length parameter.

2. Parameter c_2 is linked with nonlocal turbulent diffusion, which defines the distance of overshooting. Our study shows that overshooting distance is different for different physical quantities, and that can change several times. For example, the e-folding length of turbulent velocity and temperature fluctuation is $H/\beta \sim 1.4(c_1 c_2)^{1/2} H_P$, where H_P is the local pressure scale height and β is defined by equation (24) (Xiong & Deng 2002).

3. Parameter c_3 is a measure of the capability to restore the isotropy of turbulence through the correlation between pressure and velocity gradient. The larger c_3 is, the stronger such capability, and the turbulent convection is more isotropic (see Table 1).

A series of models of the solar convection zone with different c_1, c_2, and c_3 have been calculated.

3.1. The Anisotropy of Turbulent Velocity in Convection and Overshooting Zones

Figure 1 shows the ratio of the radial component and the horizontal one of turbulent velocity, w_r^2/w_h^2, as a function of depth (in $\log P$) in solar convection zone models with $c_3 = 1, 2, 3, 7,$ and 255 when $c_1 = 0.66$ and $c_2 = c_1/4$. The central part of the figure ($5 \lesssim \log P \lesssim 14$) is the convection zone ($L_c/L > 0$), and the two ends ($\log P \lesssim 5$ and $\log P \gtrsim 14$) are the overshooting zones ($L_c/L < 0$). As shown in Figure 1, radial motion of turbulence dominates within the convection zone, and turbulent velocity tends to become isotropic as c_3 increases. Table 1 gives numerical results (corresponding to the "flat" part of the lines in Fig. 1) of w_r^2/w_h^2 for the solar convection zone in the last row, from
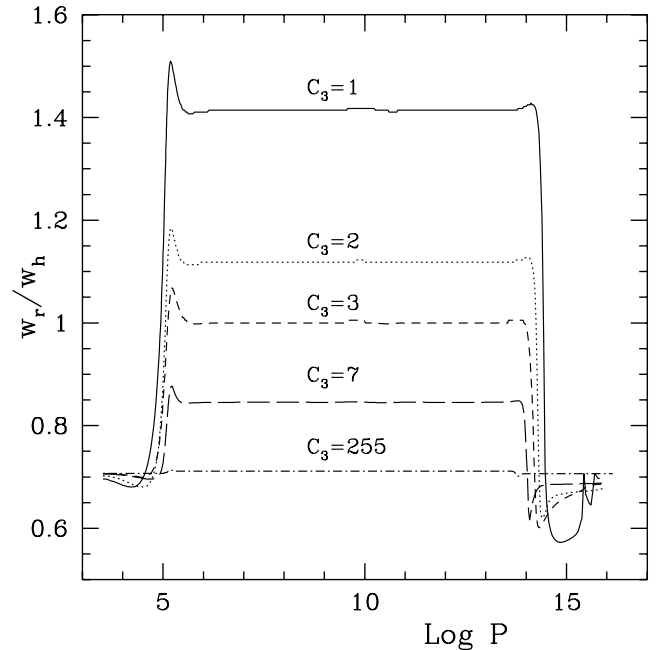

Fig. 1.—Ratio of the radial turbulent velocities to the horizontal one w_r/w_h vs. the depth for solar convective models with $c_1 = 0.66$ and $c_2 = 0.165$, but different $c_3 = 1, 2, 3, 7,$ and 255.

where one can see that the numerical results closely match those of the theoretical asymptotic analysis using the local convection treatment (the second row in Table 1).

In the upper overshooting zone, w_r^2/w_h^2 is slightly less than 0.5 (i.e., very close to isotropic turbulence), and that is almost independent of c_3. While in the lower overshooting zone, $w_r^2/w_h^2 < \frac{1}{2}$, which means that convective motion is primarily horizontal, and for decreasing c_3, w_r^2/w_h^2 tends to decrease. The difference between these two overshooting zones is very likely due to the distinct effective Peclet numbers: for the upper zone, $P_e \ll 1$, so that convection is highly inefficient there, and the superadiabatic temperature gradient $\nabla - \nabla_{ad} \sim -0.4$. In that case, a convective eddy will face a strong elastic wall when entering the upper overshooting zone, temperature drops off abruptly, and the motion of the eddy decreases and eventually bounces back. Passing through the boundary of the convective zone, the correlation of velocity and temperature jumps from $+1$ to -1. In the convective zone and the lower overshooting zone, however, $P_e \gg 1$, convection is very efficient for energy transport and $|\nabla - \nabla_{ad}| \ll 1$; convection is subadiabatic ($\nabla - \nabla_{ad} < 0$) far before reaching the lower overshooting zone. While in the lower overshooting zone, convection is subadiabatic but superradiative ($\nabla_{ad} > \nabla > \nabla_{rad}$); this is due to the fact that convective energy flux becomes negative ($L_c < 0$) in this region. The structure of the lower overshooting zone sketched by our theory is completely different from that predicted by classical nonlocal mixing-length theories (Shaviv & Salpeter 1973; Maeder 1975; Bressan et al. 1981; Zahn 1991; Monteiro et al. 2000). As commented by Petrovay & Marik (1995), such a misunderstanding in the mixing-length theories was due to the fact that nonlocal mixing-length theories assumed implicitly that turbulent velocity is fully correlated with temperature fluctuations. However, such a correlation decreases very quickly toward the lower boundary of the convective zone. Figure 2 depicts the model of the solar convective zone in terms of fractional convective flux L_c/L, the correlation of turbulent velocity and temperature R_e, and superadiabatic temperature gradient ($\nabla - \nabla_{ad}$) as functions of depth ($\log P$). Within the
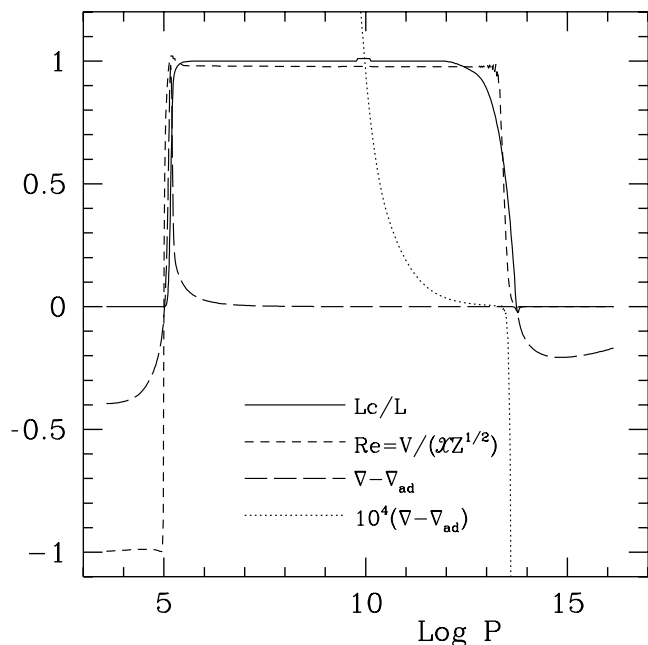
Fig. 2.—Fractional convective flux L_c/L, superadiabatic temperature gradient $\nabla - \nabla_{\mathrm{ad}}$, and the coherence between turbulent velocity and temperature $R_e = V/xZ^{1/2}$ as functions of depth for model 3.
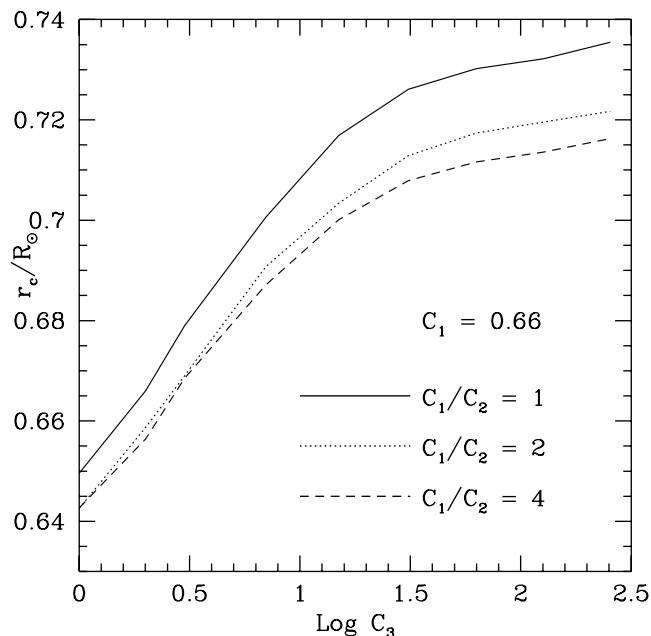

Fig. 3.—Depth of the convective zone as a function of c_3 for three sets of the solar convective zone model with $c_1 = 0.66$ and $c_2 = 0.66, 0.33$, and 0.165, respectively.

convective zone and upper part of the lower overshooting zone, $\nabla - \nabla_{\mathrm{ad}}$ is virtually zero (Fig. 2, *dashed line*). We have multiplied $\nabla - \nabla_{\mathrm{ad}}$ by 10^4 in order to make it visible in the plot (*dotted line*). It follows directly from Figure 2 that, going toward the lower overshooting zone, $\nabla - \nabla_{\mathrm{ad}}$ has been negative far away from the boundary. The difference between the models made of nonlocal and local convection theories can be used to perfectly explain the abrupt temperature rise at the lower overshooting zone of the solar convective zone (Xiong & Deng 2001), which is an observational fact provided by helioseismic inversion of the solar convective zone.

It is worth stressing here again that equation (42) is derived from the dynamic equations of turbulent velocity correlations (eqs. [12] and [17]) under the condition of neglecting the third-order correlations; therefore, the local treatment is retained. Within a convective zone, the third-order correlations can be neglected because they are relatively small compared with other terms. As such, convective motions are similar to what can be expected from a local theory. However, the third-order correlations tend to become significant near the boundary of a convective zone and within the overshooting zones and can no longer be ignored. Hence, equation (42) is not valid in such a context, as clearly demonstrated in Figure 1.

3.2. *The Effects of Anisotropy of Turbulence on the Structure of the Stellar Convective Zone*

Figure 3 shows the variations of the depth of the convection zone $r_c/R_\odot$ with respect to convective parameter c_3 in three sets of convective parameters $(c_1, c_2) = (0.66, 0.66), (0.66, 0.33), (0.66, 0.165)$, where r_c is the radius at the bottom of the solar convective zone and $R_\odot$ is the radius of the Sun. It follows from Figure 3 that convection gets deeper for smaller c_3 with given c_1 and c_2. This is because the radial turbulent velocity increases with smaller c_3 in the convective zone (see also Fig. 1), while turbulent velocity is mostly positively correlated with temperature (see Fig. 2). Therefore, $V = \overline{w'_h T'}/\bar{T}$ (and convective flux $F_c = \rho C_P T V$) grows for smaller c_3 within the convective zone.

As a result, the temperature gradient of the outermost superadiabatic region of the stellar convective zone will decrease for smaller c_3. The depth of the outer convective zone of stars is mainly fixed by the structure of the superadiabatic zone: the larger the temperature gradient in the superadiabatic zone, the shallower the convective zone. Hence, it is straightforward to conclude that the depth of the convective zone gets deeper for smaller c_3 with given c_1 and c_2. Figure 4a gives the fractional convective flux L_c/L as a function of depth in the superadiabatic zone of the model of the solar convective zone with $c_1 = 0.66$, $c_2 = c_1/4 = 0.165$, and $c_3 = 1, 3, 255$.

As shown in Figure 3, given c_1 and c_3, convection becomes shallower for larger c_2; this is due to the fact that the nonlocal convective diffusion is proportional to c_2. Therefore, more turbulent kinetic energy will be leaked to the overshooting zone on top of the convective zone for greater c_2. As a result, convective flux at the upper part of the convective zone will decrease for greater c_2, and the temperature gradient over there will increase; the convective zone becomes shallower then. Figure 4b shows the fractional convective flux L_c/L as a function of depth in three models of the solar convective zone with $c_1 = 0.66$, $c_3 = 3$, and $c_2 = 0.66, 0.33$, and 0.165, respectively.

Also from Figure 3, we can see that the anisotropy of turbulent convection has an apparent influence on the depth of stellar outer convective zones. For example, for the solar convective zone model with $c_1 = 0.66$, $c_2 = c_1/4 = 0.165$, and $c_3 = 255$, the depth of the convective zone is $r_c/R_\odot = 0.7163$, and the temperature at the bottom of the convective zone is $T_c = 2.23 \times 10^6$ K; in contrast to that, for another model with the same c_1 and c_2 but $c_3 = 3$, the depth of the convective zone is now $r_c/R_\odot = 0.6685$ and $T_c = 2.76 \times 10^6$ K; the two models are quite different indeed. The divergence of the results shows the dependence of model properties on the selection of parameters; the true value of the parameters linked with a correct model can be fixed by observations. Once we have c_3 and c_2/c_1 determined observationally or somehow theoretically, it is always possible to adjust the convective parameter c_1 so that the predicted depth of the solar convective zone matches that derived from helioseismology.
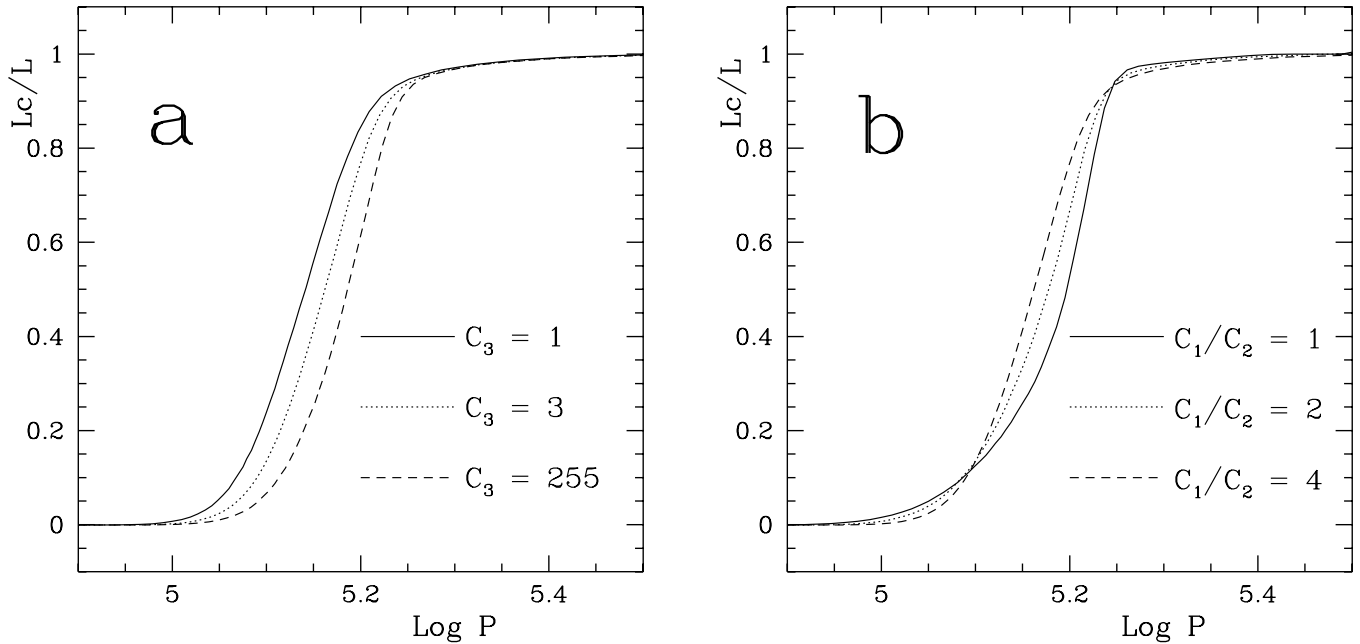
Fig. 4.—Fractional convective flux L_c/L as a function of depth of the solar convective zone model with (a) $c_1 = 0.66$, $c_2 = 0.165$, and $c_3 = 1$, 3, and 255 and (b) $c_1 = 0.66$, $c_3 = 3$, and $c_2 = 0.66$, 0.33, and 0.165.

Four models of the solar convective zone with the depth required by helioseismology (Basu 1997) are presented in Table 2; they have different combinations of convective parameters c_1, $c_2 = c_1/4$, and c_3. The relative difference of model 1 and model 3 in terms of adiabatic sound speed $\delta c_s^2/c_s^2$ and density $\delta\rho/\rho$ as functions of depth is shown in Figure 5. As shown in the plot, the two models are very similar: the relative difference between them is less than 1/1000. It is not possible to detect such a tiny difference for stars, except our Sun. Although being very small, the two models still show small deviations at the bottom of the convective zone as one can see from Figure 5. Such deviations neither are due to the numerical errors in the calculations nor result from inaccurate tuning of the parameter c_1. In fact, these two models show true fine deviations at the lower overshooting zones. For the Sun, it can be well detected through helioseismic inversion. Figures 6a and 6b show, respectively, the variations with depth of the auto- and cross-correlations of turbulent velocity and temperature fluctuations x, Z, and V in the upper and lower part of the convective zone for the two models, where the dip on the $\log|V| - \log P$ curve (where V changes its sign) is exactly the boundary of the convective zone. As shown in Figures 6a and 6b, the turbulent velocities and temperature fields of the four models are very similar within the convective zones. In the overshooting zones, however, smaller c_3 makes x, Z, and $|V|$ decrease faster. This is due to the proportionality of the e-folding lengths of both x and V to $(c_1c_2)^{1/2} = c_1/2$ (for $c_2 = c_1/4$). If one wanted to make the models with different c_3 have the same

depth of convective zones, one should also make c_1 smaller for smaller c_3.

3.3. The Effects of Anisotropy of Turbulent Convection on the Evolution of Stars

Except the surface layers, $P_e \gg 1$ holds for all cases of convection inside stars; convection is very efficient, so that the temperature gradient is almost adiabatic, i.e., $\nabla - \nabla_{ad} \ll 1$, regardless of the choice of convection parameters c_1, c_2, and c_3. It seems that convection parameters have little to do with the internal temperature-pressure structure of stars. However, this does lead to the conclusion that they have no influence on the evolution of

TABLE 2
Models of Solar Convective Zone

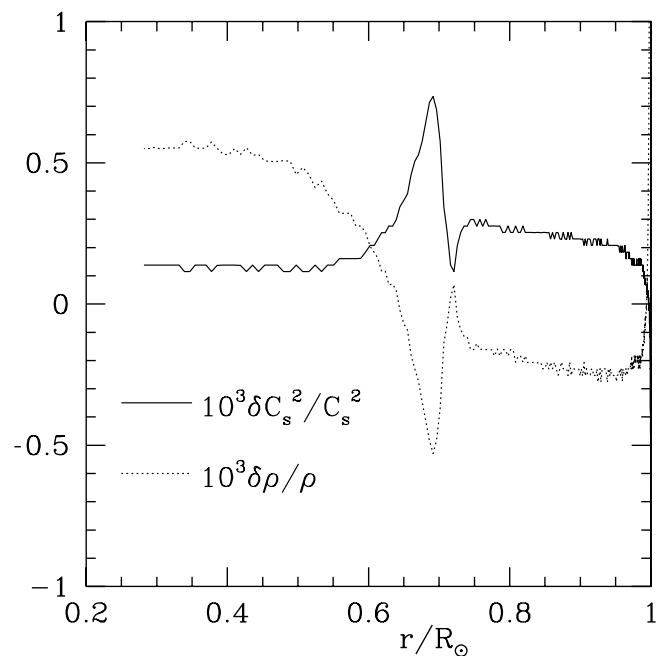| Model	c_1	c_2	c_3	$r_c/R_\odot$	T_c $(10^6$ K$)$
1................................	0.6600	0.1650	255	0.7163	2.23
2................................	0.5800	0.1450	7	0.7158	2.23
3................................	0.5200	0.1300	3	0.7163	2.23
4................................	0.4325	0.1083	1	0.7163	2.23

Fig. 5.—Relative differences in the squared sound speed and densities between model 1 and model 3 vs. $r/R_\odot$.
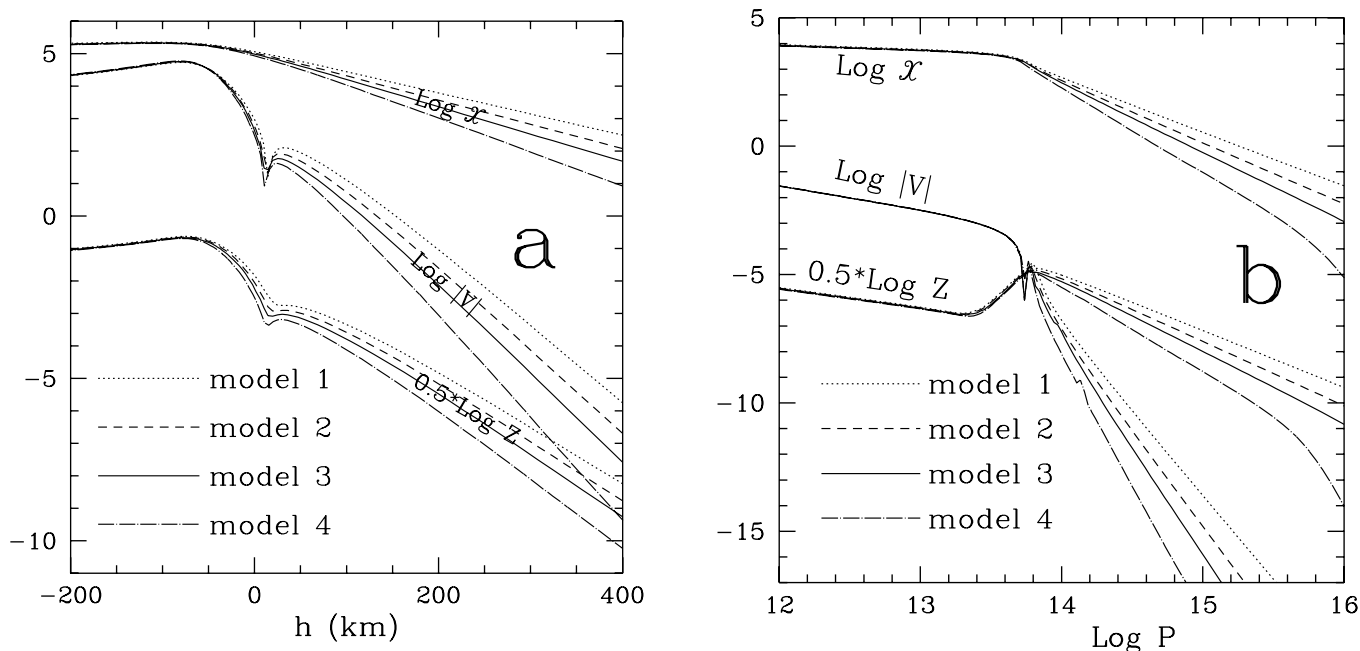
Fig. 6.—Turbulent velocity, temperature, and velocity-temperature correlation vs. depth. (*a*) In the solar atmosphere, the abscissa is the height above $\tau = 1$. (*b*) In the lower layer of the convective zone.

stars. On the contrary, c_1, c_2, and c_3 affect critically the extension of convective overshooting zone and therefore the nonlocal mixing of chemical elements inside stars and further the evolutionary properties of stars. As shown in Figures 6a and 6b, with the decrease of anisotropy parameter c_3, the convective overshooting zone retreats. To make such a prediction more convincing, we have calculated the depletion of the atmospheric lithium abundance in four models of the solar convection zone. The results are presented in Figure 7, in which the evolution curve of lithium abundance $A[\mathrm{Li}] = \log(N_{\mathrm{Li}}/N_{\mathrm{H}}) + 12$ is plotted, where N_{Li} and N_{H} are solar atmospheric atomic number densities of lithium and hydrogen, respectively; the initial lithium
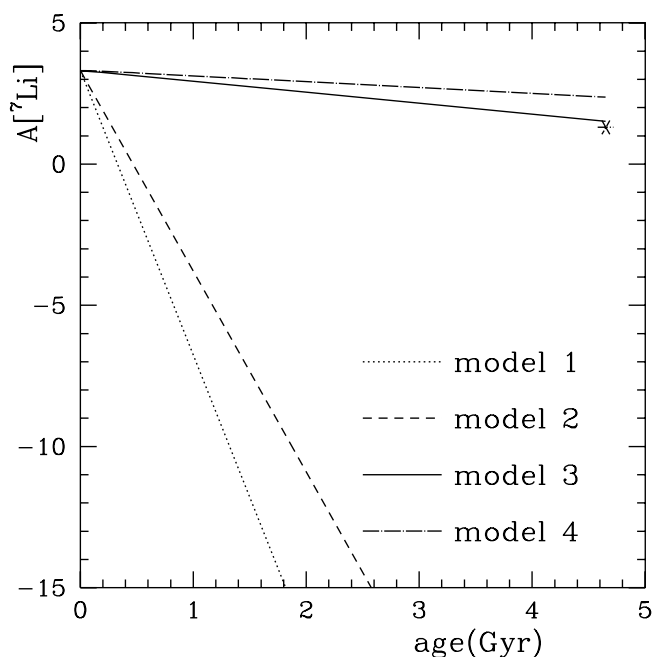
abundance (defined above) is taken to be 3.3. The asterisk shows the current location of the Sun. It follows from Figure 7 that the depletion of solar atmospheric lithium abundance increases very quickly with growing c_3, although all four models of the convective zone have the same depth of the convection zone. This is apparently due to the fact that the lithium abundance depends sensitively on the extension of the overshooting zone, which, in turn, is a function of c_3. As one can also see from Figure 6b, the downward attenuation of turbulent velocity x increases quickly with smaller c_3 at the bottom overshooting zone, and this is why the depletion of lithium slows down for smaller c_3.

It is seen also from Figure 7 that the location of the current Sun sits very closely on the lithium abundance depletion curve of model 3. This implies that it is promising to explain the lithium depletion problem of the Sun and solar-type stars using the mechanism of convective overshooting. More theoretical computational efforts should be put forward to verify such an idea, including considering the evolutionary effects of the Sun and stars. This has exceeded the purpose of the current work and is not dealt with here.

3.4. *A Comparison with Observations of the Solar Convective Zone*

Being distinctly different from the nonlocal mixing-length theories (e.g., Spiegel 1963; Ulrich 1970a, 1970b), our nonlocal convection models have the following characteristics:

1. Within the convective overshooting zone, turbulent velocity and temperature fluctuations drop off exponentially with respect to pressure. Crossing the boundary of the convective zone, the turbulent velocity–temperature correlation changes its sign; i.e., convective flux becomes negative in the overshooting zone.

2. Within the convective zone, turbulent velocity is mainly radial, while in the overshooting zone, it becomes nearly isotropic; the horizontal component is about $\sqrt{2}$ times the radial component.

Fig. 7.—Depletion of lithium abundance with time for solar convection models 1–4.

The study of the granular structure of the Sun has a long history. Table 3 lists three groups of studies on the variation of

TABLE 3
OBSERVATIONAL AND THEORETICAL MODEL OF THE SOLAR ATMOSPHERE VELOCITY FIELD

SOURCE	RADIAL				HORIZONTAL			
	V_1	H_1	V_2	H_2	V_1	H_1	V_2	H_2
Keil & Canfield	1.45	140	...	...	2.70	230	...	...
Nesis & Mattig	1.05	95	0.115	270	1.1	75	0.2	290
Komm, Mattig, & Nesis	1.35	70	0.247	600	2.10	85	0.210	400
Model 1..	1.64	67	...	...	1.68	67	...	...
Model 2..	1.50	58	...	...	1.50	58	...	...
Model 3..	1.34	52	...	...	1.34	52	...	...
Model 4..	1.02	40	...	...	1.03	40	...	...

the velocity field of solar granules with respect to height. Similar methods have been adopted in those studies, assuming that the variations of the velocity field with height can be fitted using the following analytical formula (Nesis & Mattig 1989):

$$v(h) = V_1 \exp(-h/H_1) + V_2 \exp(Z/H_2).$$

The observed velocity field of granules can be expressed in terms of the velocity weighting function $w_v(h)$ (Canfield 1976),

$$V_{\mathrm{gran}} = \int_{-\infty}^{\infty} w_v(h)v(h)\,dh.$$

By measuring the granular velocity field with spectral lines formed at different heights (Keil & Canfield 1978; Komm et al. 1991), or with the same spectral line having different residual intensities (Nesis & Mattig 1989), one can determine the parameters H_1, H_2, V_1, and V_2. By observing velocity fields from the limb to the center of the Sun, one can measure the distribution of radial and horizontal components of the velocity field with respect to height. Table 3 gives the parameters H_1, H_2, V_1, and V_2 of each member of the research group, while Figures 8a

and 8b show the distributions of radial and horizontal components of the solar granular velocity field with respect to height as derived from their parameters, respectively.

The distributions of the radial and horizontal components of turbulent velocity of our theoretical models are plotted in Figures 9a and 9b, respectively. The fitted parameters V_1 and H_1 are also presented in Table 3. Comparing our model with observations, we found out that the turbulent velocity decreases quickly with height at the lower and intermediate layers of the photosphere ($h \leq 200$ km). The trends are the same for both cases; however, the theoretical prediction favors a much faster decrease than observed. In the upper layers ($h \geq 200$ km), the observations of Nesis & Mattig (1989) and Komm et al. (1991) show that the velocity field changes slowly with height and seems slightly increasing toward the outside. This is possible by not representing convective overshooting and ought to be attributed to some other physical processes not yet known to us (Komm et al. 1991).

Comparing the theoretical ratio of radial and horizontal components of turbulent velocity w_r/w_h with that of observations, no similarity is found. According to our theoretical predictions, $w_r/w_h \geq 0.71$ in the convective zone ($h \leq -10$ km), while in the overshooting zone it gradually approaches isotropic ($w_r/w_h \leq 0.71$). This is not at all shown by observations. As shown in
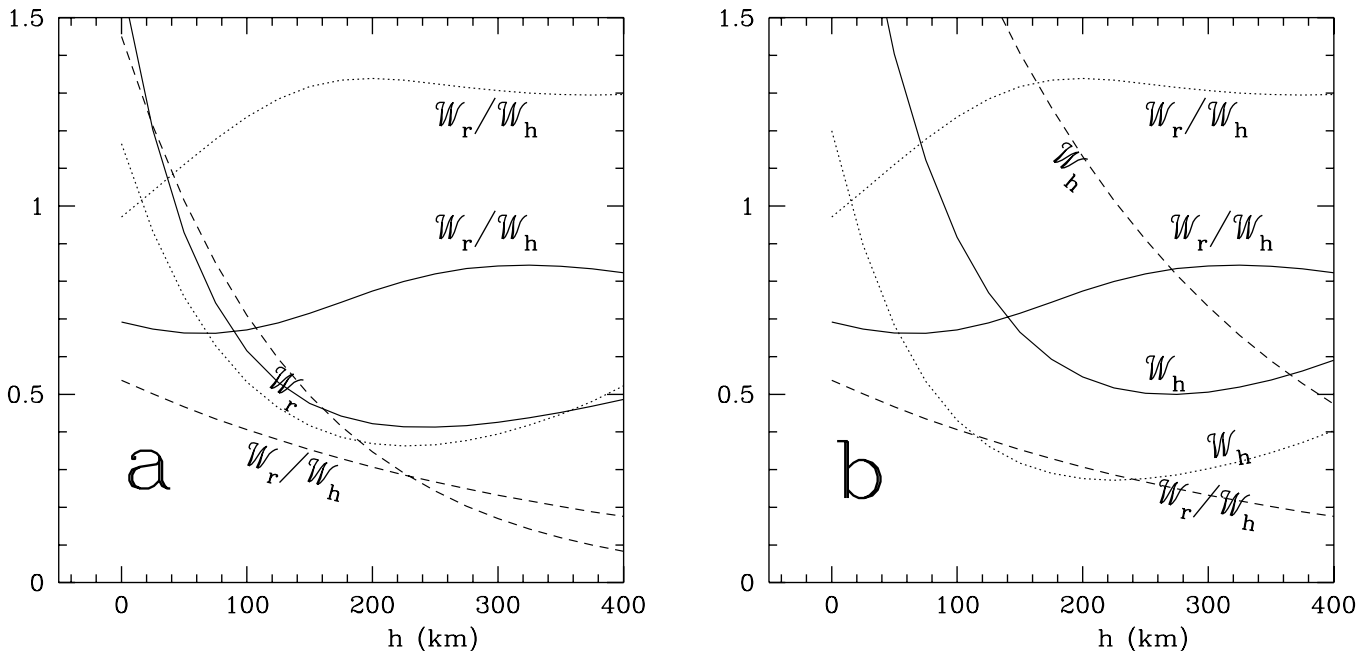

FIG. 8.—(a) Vertical and (b) horizontal components of granular rms velocity calculated from spectrographic observations of the Sun vs. height about $\tau_{5000} = 1$. The ratios of the vertical component to the horizontal one of turbulent velocity are also plotted. The solid lines are taken from Komm et al. (1991), the dotted line from Nesis & Mattig (1989), and the dashed lines from Keil & Canfield (1978).
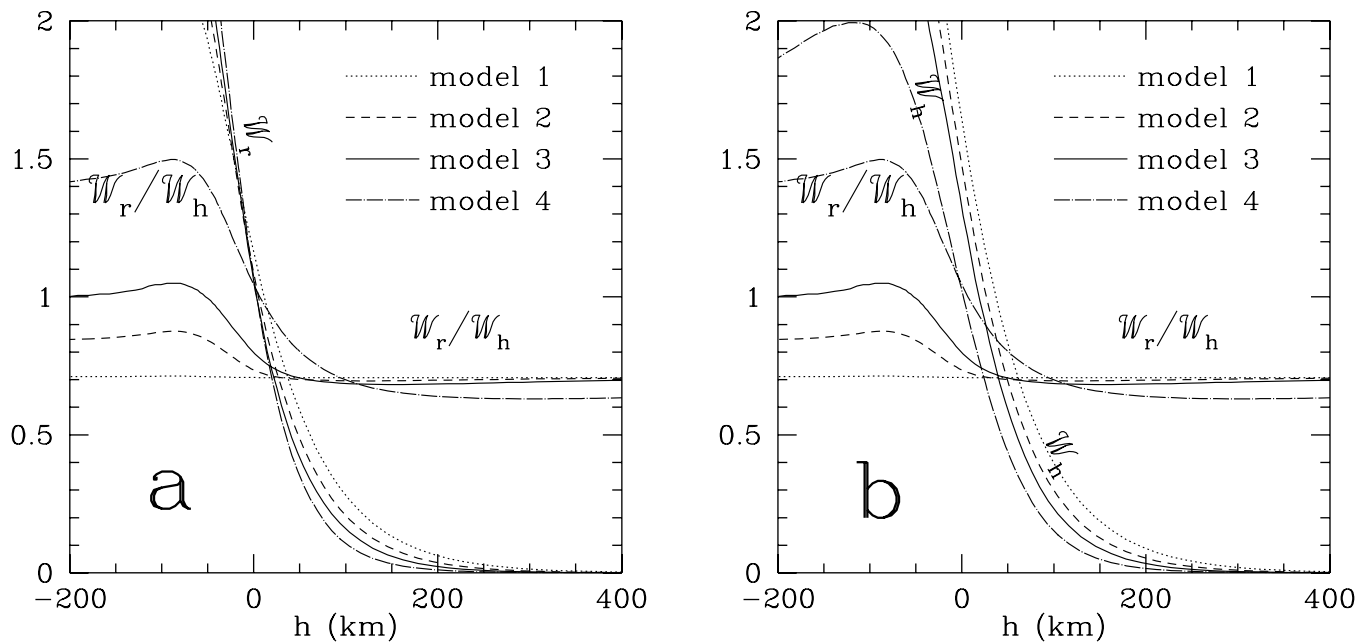
FIG. 9.—(a) Vertical and (b) horizontal components of turbulent velocity vs. height above $\tau = 1$ for solar convection models 1–4.

Figure 8, w_r/w_h in the three sets of observational data are very different, which implies that such observations are still not convincing enough to make a conclusive judgment on our model. It is known that there are still large uncertainties in the observation of the velocity field of solar granules:

1. The observed velocity field contains at least two components: the velocity field of granules and that of solar 5 minute oscillations. Time series photometry is needed in order to completely decompose the two components (Keil 1980; Bässgen & Deubner 1982), in that the solar 5 minute oscillation can be cleared out on the k-w diagram of the solar oscillation analysis. However, there are no such long time series observations for the granular velocity field. A regular practice is to set a minimum wavenumber k_0 of the granular velocity field, assuming that all velocity components with $k < k_0$ are due to solar oscillations and that the remaining modes with $k \geq k_0$ are the real granular velocity field. Such discrimination is obviously not clean, which removes velocity fields of large-scale granules on the one hand and on the other hand keeps the components of solar oscillation in the velocity field with $k \geq k_0$ and of course that of observational noise.

2. The observations of the solar velocity field are distorted due to instrumental noise and the atmospheric seeing. Even at a perfect seeing condition, the uncorrected value differs from the corrected one by at least a factor of 2, as concluded by Komm et al. (1991).

Before any reliable observations come in, direct hydrodynamic simulations should be regarded as a more realistic constraint on our theory and the selection of the parameter of anisotropic convection c_3.

3.5. *A Comparison with Hydrodynamical Simulation Results*

The results of a hydrodynamic simulation are presented here as a comparison. The vertical profiles of w_r/w_h (*solid line*), w_r (*dashed line*), and w_h (*dot-dashed line*) from a three-dimensional simulation of convection with upward overshooting are shown in Figure 10. The abscissa is the depth in $\ln p$ (decreases with height); the radiation-convection transition boundary is at 0. In the convective region, the radiative gradient ∇_r is much larger

than the adiabatic gradient ∇_{ad} (=0.4). In the radiative region, ∇_r has the value 0.2. Both the stable and the unstable regions contain about 4 pressure scale heights. Toward the top and bottom boundaries, w_r and thus w_r/w_h drop off quickly due to the nonpenetrative boundary conditions assumed in the model and therefore are not real. The region $3 > \ln p > 0$ corresponds approximately to the upper layer of the solar convection zone. In Figure 1, w_r/w_h reaches a maximum value of about 0.9. From Table 1, it can be seen that this is compatible with a value of c_3 between 3 and 7. In the overshoot region, however, w_r/w_h is around 0.2, which is far smaller than the predicted value of the theory. How should we interpret such distinct properties of the convective and overshooting zones? The anisotropy depends on the nature and the strength of the stratification force on the fluid elements, namely, the factor $\nabla - \nabla_{ad}$. Deep inside the convective zone, $\nabla - \nabla_{ad}$ is positive and very small ($\ll 1$); therefore, the anisotropy of the velocity field favors the radial direction due to
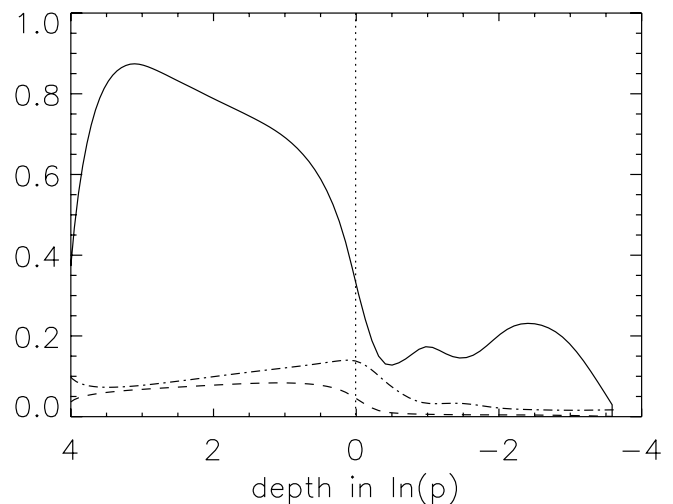

FIG. 10.—Vertical profiles of w_r/w_h (*solid line*), w_r (*dashed line*), and w_h (*dot-dashed line*) from a three-dimensional simulation of convection with upward overshooting. The abscissa is the depth in $\ln p$ (decreases with height); the radiation-convection transition boundary (*vertical dotted line*) is at 0.

buoyancy acceleration, but the stratification force is mild and a modest enhancement of w_r/w_h is created. However, in an overshooting zone with $\nabla - \nabla_{ad} \approx -0.2$, the antibuoyancy effect dominates over the isotropizing effect of the turbulent pressure–velocity gradient correlation, and a low value of w_r/w_h appears. This is particularly significant in the overshoot region right next to the convection-radiation transition layer (w_r/w_h is minimized).

It follows from equations (12) and (14) that in our nonlocal convection theory, the radial turbulent diffusion coefficient is proportional to $w_r \Lambda$ (Λ being the diffusion length). We have assumed that the diffusion length is proportional to the local pressure scale height, i.e., $\Lambda = \sqrt{3}/4\Lambda_1 = \sqrt{3}/4c_2 H_P = \sqrt{3}c_2 r^2 P/4GM_r\rho$; the parameter c_2 can be fixed using the observational solar lithium abundance. In order to secure our nonlocal convection model in terms of both the observational solar lithium abundance and the helioseismic depth of the solar convective zone, we need to take $c_2 \approx c_1/5$ (Xiong & Deng 2002). According to the theory of turbulence, the turbulent diffusion length Λ should have a similar magnitude as the linear size of the energy-containing eddies, so that c_1 and c_2 ought to be similar. A small value of c_2/c_1 derived by the observational constraints cannot be understood easily. If one accepts the picture offered by the hydrodynamical simulation, in the overshooting zone, the radial component of turbulence w_r is much smaller than the horizontal one w_h, and then the turbulent diffusion coefficient Λw_r can be made smaller without a large reduction of the diffusion length Λ (or the convection parameter c_2). This may reconcile or even remove the problem of requiring c_2/c_1 to be small.

4. CONCLUSIONS

We have presented in this paper a simple anisotropic nonlocal theory of convection, which we have used to analyze the anisotropy of the convective turbulence and its possible consequences on the internal structure and evolution of stars. The results are concluded as follows:

1. The anisotropy of turbulence has hardly any important effects on the internal structure of stars.

2. The anisotropy of turbulent convection seriously affects the nonlocal convective mixing process and therefore the evolution of stars.

3. Inside the convection zone, both the simulation model and our simple nonlocal theory produce an anisotropy that favors the radial direction (i.e., $w_r/w_h > 0.71$). By considering lithium abundance, the convection parameter $c_3 = 3$ is preferred. This is also corresponding to the most unstable convective mode from a linear stability analysis of the convective zone (Unno 1961). That seems to be incompatible (being too small) with the value indicated by the three-dimensional model (between 3 and 7). However, the results of the simulation presented here are based on a relatively shallow convection zone (about 4 pressure scale heights in depth). In the simulation of a deeper convection zone (Chan & Sofia 1996), which contains about 7 pressure scale heights, w_r/w_h reached 1.16. The ratio is close to what can be expected with $c_3 = 3$. The older simulation, however, did not include a substantial overshoot layer, and the small aspect ratio of the computed domain (1.5 vs. the current 6) might have an effect on the velocity ratio. Further simulations are needed to obtain a more reliable estimate for the asymptotic value of this quantity. The current comparison with simulations can only be viewed as preliminary and qualitative.

4. In the overshoot zone, our theory generally predicts a velocity ratio below 0.71, showing that the horizontal velocity component becomes dominant. This is an important feature due to the nonlocal nature of the theory, as equation (42), based on neglecting the nonlocal effects, limits w_r/w_h to above 0.71. In comparison with the simulation model ($w_r/w_h \sim 0.2$), the theoretical predictions seem to be too large. The differences call for further investigation.

5. Within an overshooting zone, $w_r/w_h \ll 1$ would greatly reduce the turbulent diffusion coefficient there. This may help to avoid the need to make c_2/c_1 (diffusion length vs. dissipation length) small in our anisotropic turbulent diffusion theory.

REFERENCES

Bässgen, M., & Deubner, F. L. 1982, A&A, 111, L1
Basu, S. 1997, in IAU Symp. 181, Sounding Solar and Stellar Interiors, ed. J. Provost & F.-X. Schmider (Dordrecht: Kluwer), 137
Böhm-Vitense, E. 1958, Z. Astrophys., 46, 108
Bressan, A., Bertelli, G., & Chiosi, C. 1981, A&A, 102, 25
Canfield, R. C. 1976, Sol. Phys., 50, 239
Canuto, V. M. 1993, ApJ, 416, 331
———. 1997, ApJ, 482, 827
Chan, K. L., & Sofia, S. 1996, ApJ, 466, 372
Gough, D. O. 1969, J. Atmos. Sci., 26, 448
Hinze, J. O. 1975, Turbulence (New York: McGraw-Hill)
Keil, S. L. 1980, ApJ, 237, 1024
Keil, S. L., & Canfield, R. C. 1978, A&A, 70, 169
Komm, R., Mattig, R. W., & Nesis, A. 1991, A&A, 243, 251
Latour, J., Spiegel, E. A., Toomre, J., & Zahn, J. P. 1976, ApJ, 207, 233
Ludwig, H.-G., Freytag, B., & Steffen, M. 1999, A&A, 346, 111
Maeder, A. 1975, A&A, 40, 303
Monteiro, M. J. F. G., Christensen-Dalsgaard, J., & Thompson, M. J. 2000, MNRAS, 316, 165
Nesis, A., & Mattig, W. 1989, A&A, 221, 130

Petrovay, K., & Marik, M. 1995, in ASP Conf. Ser. 76, GONG '94: Helio- and Astero-Seismology from the Earth and Space, ed. R. K. Ulrich, E. J. Rhodes Jr., & W. Däppen (San Francisco: ASP), 216
Rotta, J. C. 1951, Z. Phys., 129, 547
Shaviv, G., & Salpeter, E. E. 1973, ApJ, 184, 191
Spiegel, E. 1963, ApJ, 138, 216
Ulrich, R. K. 1970a, ApJ, 162, 993
———. 1970b, Ap&SS, 7, 183
Unno, W. 1961, PASJ, 13, 276
Xiong, D. R. 1977, Acta Astron. Sinica, 18, 86
———. 1978, Chinese Astron. Astrophys., 2, 118
———. 1979, Acta Astron. Sinica, 20, 238
———. 1980, Chinese Astron. Astrophys., 4, 234
———. 1986, A&A, 167, 239
———. 1989a, A&A, 209, 126
———. 1989b, A&A, 213, 176
Xiong, D. R., Cheng, Q. L., & Deng, L. 1997, ApJS, 108, 529
Xiong, D. R., & Deng, L. 2001, MNRAS, 327, 1137
———. 2002, MNRAS, 336, 511
Zahn, J. P. 1991, A&A, 252, 179